International Journal of Sciences

Research Article

Turbidity Removal Efficiency of Clay and a Synthetic af-PACl Polymer of Magnesium Hydroxide in AMD Treatment

Ntwampe, I.O.[1]; Waanders, F.B.[1]; Fosso-Kankeu, E[1]; Bunt J.R.[1]

[1]School of Chemical and Minerals Engineering, North West University, Faculty of Engineering, North West Province, Potchefstroom Campus, South Africa

Abstract: In this study five 200 mL acid mine drainage (AMD) samples were treated with 5g clay (bentonite) alone or mixed with 0.1 M Al^{3+} in $AlCl_3$ and 0.1 M Mg^{2+} in $Mg(OH)_2$ polymer. The AMD samples were poured into five 500 mL glass beakers and dosed with 5 g/L of clay in a jar test, (250 rpm for 2 minutes and reduced to 100 rpm for 10 minutes) and the samples were allowed to settle for 1 hour after which the pH, conductivity, turbidity, dissolved oxygen (DO) and oxidation reduction potential (ORP) were measured. In the next step, 200 mL of the supernatant was poured into five 500 mL glass beakers and dosed with a af-PACl (acid-free polyaluminiumchloride) polymer of 0.1 M Al^{3+} in $AlCl_3$, mixed with 0.1 M Mg^{2+} in $Mg(OH)_2$, and treated in a similar manner in a jar test, settled for 1 hour, after which similar measurements were conducted, depicted as experiment (A). Another similar set of experiments was conducted, where the AMD sample was dosed with a polymer of 5 g of clay, 0.1 M Al^{3+} in $AlCl_3$ and 0.1 M $Mg(OH)_2$ in a jar test. Similar measurements were conducted after 1 hour of settling, depicted as experiment (B). The results showed that the addition of the clay to the AMD sample as a reagent (A) or a polymeric component (B) does not affect the turbidity removal, but the rate of hydrolysis (pH changing pattern) and ORP are affected. The experimental results showed that there is a correlation between the ORP and the pH, and also showed that oxidation takes place during the destabilization-hydrolysis process. The results also showed that the conductivity plays a role during the destabilization-hydrolysis process, i.e. correlation between changing rate of the conductivity and the turbidity.

K**eywords:** mixing, disperse, turbidity, multivalent, pH, turbidity

1.0 Introduction

Conventional wastewater treatment using inorganic coagulants is a common practice because aluminium, one of the reagents utilized in the process is in abundance and has also exhibited desirable effectiveness in the wastewater treatment. On the other hand, the use of polymeric flocculants over inorganic polyelectrolytes, such as poly-aluminium complexes, gives significant advantages when the water has a high concentration of suspended solids; the concentration of the polymeric flocculent is lower, the resulting sludge is more compact and there is less coagulant left in the water after treatment (Stoll, 2013). However polymeric flocculants are not always used in a rational way for optimal flocculation due to the natural fluctuations and heterogeneity of the water composition (e.g., pH, ionic composition), suspended particle concentration and corresponding physicochemical properties (e.g., sizes, shapes, surface charges). The main objective in the present study is to investigate the impact of the polymer which contains clay and $Mg(OH)_2$ with $FeCl_3$ on the destabilization-hydrolysis process for an AMD sample. An improved understanding of the interaction mechanisms between flocculants and the suspended material is also often necessary. Since most of the flocculation mechanisms are mainly driven by electrostatic interactions, the polymer and aggregate electrostatic charges are key parameters to take into consideration. Although the utilization of aluminium in wastewater treatment has been associated with health problems in potable water supplies, the United Kingdom promulgated concentration limits in 1989 to alleviate any inevitable health hazards. The most appropriate utilization of aluminium salt, $AlCl_3$ is in the treatment of AMD, a health and environmental hazardous wastewater which is generated mainly from gold and

Published at: http://www.ijsciences.com/pub/issue/2015-09/
DOI: 10.18483/ijSci.757; Online ISSN: 2305-3925; Print ISSN: 2410-4477

Oupa Ntwampe (Correspondence)
ontwampe@gmail.com
+27 18 299 1988, Fax: +27 18 299 1988

coal mining and cleaning (Gupta, 2007, Huang *et al.*, 2008, Hower *et al*., 2008, Cravotta *et al*., 2008, Silva *et al*., 2009a, Galatto *et al*., 2009 and Silva *et al*., 2010a). The application in the treatment of AMD is because its effluent is not for potable supplies, but moreover that the$AlCl_3$ is mixed with $Mg(OH)_2$ to form an af-PACl polymer. It is imperative to employ an economically viable technique in the treatment of AMD because of its voluminous capacity. The AMD is derived from the oxidation of pyrite by oxygen in aqueous medium as shown by Eq. 1:

$$2\ FeS_2 + 7\ O_2 + 2\ H_2O \rightarrow 2\ Fe^{2+} + 4\ SO_4^{2-} + 4\ H^+ \quad (1)$$

Druschel (2003) stated that the pyrite can further be oxidized by Fe^{3+}, a ferric ion which is formed by oxidation of Fe^{2+}, as represented by Eq. 2:

$$FeS_2 + 7\ Fe^{3+} + 13\ H_2O \rightarrow 8\ Fe^{2+} + 0.5\ S_4O_6^{2-} + 6\ H^+ \quad (2)$$

According to Eqs. 1 and 2, it is envisaged that there is a high volume of AMD generated as oxidation of FeS_2 occurs in two reactions. Notwithstanding, the chemical reactions (Eqs. 1 and 2), which results in the production of AMD, bacterial oxidation is also inevitable, and occurs at pH values of less than 3.5.

AMD contains different minerals and also has a high ionic movement, which results in a highly reactive tendency (Skalny *et al*., 2001, Niesel *et al*., 2005, Edwards *et al*., 2007, Niesel *et al*., 2008, Niesel *et al*., 2008, Firer, 2008 and Sinha *et al*., 2013). A lot of research has been conducted on AMD and covers a diversified technological approach such as distillation, reverse osmosis, carbon nanotubes, Fenton's reagent, wet oxidation, advanced oxidation and coagulation-electro oxidation. These techniques are complex, incur high costs and do not cover a wide range of the wastewater poor quality. Apart from new technologies, lime-, dolomite-neutralization, iron oxidation, gypsum crystallization and activated carbon are common treatment techniques (Feng *et al*.,2000, Geldenhuys *et al*., 2001, Maree *et al*., 2004, Naicker *et al*., 2003, Semerjian *et al.*, 2003, Chang *et al*., 2004, Watten *et al*., 2005, Akcil *et al*., 2006, Kurniawan *et al*., 2006, Sabah *et al*., 2006, Herrera *et al*., 2007, Petrik *et al*., 2003, Meghzili, 2008, Burgess *et al*., 2009 and Sibrell *et al*., 2009). There are more complicated technologies such as co-treatment of AMD solution with municipality wastewater using activated sludge (Bratby, 2006 and Santos *et al*., 2010). Sewage effluent with relatively high concentrations of suspended solids may enhance iron oxyhydroxide precipitation by encouraging iron, which is often present in high concentrations in AMD, to form flocs (Johnson *et al*., 2006, Neto *et al*., 2010 and Winfrey *et al*., 2010). Phosphate which is present in high concentrations in sewage effluent, can be sorbed onto the iron oxyhydroxide precipitates (Sibrell *et al*., 2009; Wei *et al*., 2009 and Wei *et al*., 2010), or react with aluminium to form hydroxyl-phosphates (Johnson *et al*., 2006a and Johnson *et al.*, 2006b). Some other researchers such as Metcalf *et al*., (2003), Amuda *et al*. (2006) and Bolto *et al*. (2007) Molony, (2005), Amuda *et al*. (2006) and Ghaly *et al*. (2006) employed their technologies in wastewater clean-up, an approach which is also applicable to AMD.

Lime neutralization is popular and employed in AMD treatment, but the disadvantage is that it cannot remove certain minerals such as arsenic and molybdenum. Their removal requires co-precipitation using metal salts such as iron as Fe^{3+}, (Aube *et al*., 2003). Scaling poses another problem occurring during lime neutralization of AMD where the pH is elevated to precipitate certain metals. Controlling the pH to a typical value of 9.5 allows metals such as iron (Fe) and zinc (Zn) to precipitate. Other metals such as nickel (Ni) and cadmium (Cd) require a higher pH (in a range of 10.5 to 11.0) to effectively precipitate as hydroxides (Aube *et al*., 2003). Lime dosing can be extended to higher density sludge (HDS) processing. The precipitates are formed onto existing particles which are recycled within the process to create larger and denser particles that can settle and compress better than the typical precipitates (Aube *et al*., 2003).

The physico-chemical properties of the wastewater play a pivotal role during wastewater (AMD) treatment, as they interact amongst themselves to transform the metals/compounds to another phase and the reaction efficiency of reagents which are dosed to wastewater treatment (coagulation-flocculation process) determines the quality of the treated effluent. Coagulation-flocculation is a process which leads to nucleation, crystal growth and aggregation of the destabilised suspended particles in the solution (Kemmer, 1988, Sincero *et al*., 2003, Sharp *et al*., 2006 and Fabris *et al*., 2008)). It is also suggested that the effectiveness of the three processes determines the settling of the turbid material, resulting in optimal adsorption. The hypothesis adopted in this study states that the effectiveness of wastewater treatment is more associated with the rate of the destabilization, hydrolysis, collision, velocity gradient, settling velocity and nucleation, a concept

which is corroborated by the study conducted by Ntwampe *et al*., (2015), on AMD using synthetic acid-free inorganic polymers. Mixing, a process which induces the destabilization, hydrolysis and collision (during and after stirring), also plays a pivotal role during wastewater treatment (Freeze *et al*., 2001, Goldberg *et al*., 2002, Aysegul *et al.*, 2002, Duan *et al*., 2003, Swartz *et al*., 2004, Aboulhassan *et al*., 2006 and Syed *et al*., 2012).

A choice of an effective coagulant/flocculent is very significant as it has to destabilize the colloidal suspension. Destabilization is a process where a stable colloidal suspension occurs, which is caused by the equilibrium state between van der Waals forces of attraction and electrostatic forces of repulsion. The ionic charges from these forces form two layers namely, diffuse double and stern layers which form electrical double layer (EDL). An EDL (Fig. 1), plays a pivotal role during destabilization-hydrolysis during the coagulation process (Cheng, 2002, Sincero *et al.*, 2003, Eikebrokk, 2007 and Widerska-Broz *et al*., 2009). The reactivity of the coagulant is determined by its strength to compress the EDL. Helmholtz (1879) discovered the EDL and stated that it is formed by a layer of positive ions which surrounds the central negative ions and the mixture of positive and negative ions bound together by coulomb forces in a diffuse layer (Lee, 2001, Pratt *et al*., 2007, Haselberg, 2009, Kosmulski, 2004, Cosgrove, 2005, Crittenden *et al.*, 2005, Ananikov *et al*., 2005, Bratby, 2006 and Scholtz, 2010). These layers contain counter ions which keep the colloidal suspension in a same state indefinitely (Duan *et al*., 2002 and Binnie *et al*., 2003 and Fig. 1). The electrostatic potential in the shear plane (i.e. potential that exists between the bulk liquid and an envelope of water that moves with the particle) is expressed by Eq. 3.

$$Z_n = \frac{4\pi q d}{D} \qquad (3)$$

q = charge on the particle, d = thickness of the layer surrounding the shear plane and D = dielectric constant of liquid.

The force field of like charges in an aqueous solution (Fig. 1) come closer and the two forces, namely the electrostatic (repulsive) or van der Waals (attractive) force acts on them. In the case of the electrostatic force, the repulsive force created by the diffused counter ion atmosphere surrounding each colloid, decreases roughly exponentially with increasing distance between particles.
The electron matrix and arrangement of the ions around an aqua-colloid (determinants of the rate of the destabilization-hydrolysis) determine the stability of the colloidal suspension, electrical double layer and the size of the aqua-colloids. A double layer is formed by the diffuse layer which is concentrated with the positive and negative charges, and the layer of positive charges around the central colloid. A stern layer separates the diffuse layer and those positive charges around the central colloid, which is surrounded by the negative charges (Field *et al*., 1988). The double layer is the part of the aqua-colloid which determines the rate of the destabilization of the colloidal suspension for the induction of well-developed flocs. According to the Gouy-Chapman model, the potential distribution is a flat double layer as described by Eq. 4:

$$\frac{d\hat{}2\psi}{dx\hat{}2} = -\frac{\rho}{\varepsilon} \qquad (4)$$

ψ = potential at a point in the diffuse layer versus infinity at the bulk solution, x = charge density at the same point, ρ = density and ε = permittivity. In Eq. 4 the charge density at the potential ζ is described by Eq. 5.
The number of positive and negative ions in the diffuse layer is distributed according to the Maxwell-Boltzmann distribution (Eq. 6 for cations and Eq. 7 for anions):

$$\rho - ze\,(n_+ - n_-) \qquad (5)$$

$$n_+ - n- * \exp\left(\frac{ze\psi}{kT}\right) \qquad (6)$$

$$n_+ - n- * \exp\left(-\frac{ze\psi}{kT}\right) \qquad (7)$$

n+ and n- = are respective numbers of positive and negative ions per unit volume at the point where potential is ψ, n_0 = the concentration of ions at the infinity (bulk solution), z = the valence of the ions, e = the charge of electron, k = Boltzmann's constant and T = temperature.

The potential of the particle surface versus the bulk solution is called the Nernst potential (ψ_0). The outer Helmholtz plane (OHP) is found between the inner layer and the outer layer, which has potential of the particle surface versus bulk solution. However, this potential cannot be directly measured and therefore a common parameter, which depicts the surface charge of the colloid, is surface-potential (ψ_ζ), which is the electrical potential between the plane of shear and the bulk solution. The diffuse part of the double layer is analogous to the plate condenser. Even though in reality the double layer extends to infinity, the Debye-Hückel length, K^{-1}, is used to describe the thickness of the double layer Field *et al*., (1988), expressed by Eq. 8.

$$K^{-1} = \frac{0.0304}{\sqrt{I}} \quad (8)$$

K^{-1} = Debye-Hückel length (nm) and I = ionic strength (mol/L)

In the present study, an acid-free polymer of $AlCl_3$ and $Mg(OH)_2$ was prepared, which was also mixed with bentonite clay and dosed in each AMD sample. Unlike the costly commercial polymers (PFCl or PACl) which are prepared by partial hydrolysis of acidic aluminium chloride or ferric chloride solution in a special reactor, the polymers utilized in this study (clay, $AlCl_3$ and $Mg(OH)_2$) are easy to prepare and affordable as they are prepared by directly mixing the reagents and are then ready for use.

Kleijn *et al*., 1982 suggested that materials such as clays, which are capable of swelling in aqueous media, form a gel layer on the surface that is conductive but electrokinetically inactive. Other theories have suggested mobility of ions in the Stern layer (Urban *et al*., 1935) and conduction by ionisable surface hydroxyl groups (Holmes et al., 1965). These theories may be valuable in explaining the removal of impurities from the AMD, which is based on differences in the surface properties of the colloidal suspension because the phenomenon of this nature depends on the development of the potential difference between the solution and the reagents (coagulants/flocculants) when the two phases are in contact. There are several ways to generate this effect in aqueous systems due to the counterionic charge effect. The dipolar property of water molecules ($H^{\delta+}$-$OH^{\delta-}$), which is caused by the angle of 107^0C between the proton and the hydroxyl ions (Weber, 1972), may be oriented at the interface, thus creating a potential difference (Parra-Barraza *et al*., 2003, Darekh *et al*., 2004 and Doymus, 2007). Ions or excess electrons in one or both phases give rise to a non-uniform distribution of electric charges at the interface between the phases. Furthermore, in the development of a surface charge that exists on the solid surface, whether by ion adsorption from the liquid phase on the particle or ionization of groups, the surface acquires a potential with respect to the solution.

Apart from commonly employed parameters in AMD treatment such as the pH, conductivity and turbidity, the effect of the dissolved oxygen (DO) and oxidation reduction potential (ORP) are investigated in the present study. The DO has been used as a controlling and/or monitoring parameter for many other different treatment systems such as high sulphate wastewater treatment systems (Khanal *et al.*, 2003 and Khanal *et al.*, 2006), activated sludge systems (Li *et al.*, 2004) and nutrient removal systems (Kishida *et al*. 2003; Akın *et al*., 2005). Although the ORP has not been employed in AMD treatment, Khanal *et al*., (2003) investigated its effect in controlling sulphide, since high sulphide concentrations can often lead to poor performance and eventual process failure of an anaerobic treatment system. They found that when oxygen was added to raise the ORP from -230 to -180 mv, the dissolved sulphides were reduced to undetectable levels at all influent sulphate concentrations (Khanal *et al*., 2003).

2.0 MATERIALS AND METHODS

In this study, coagulation-flocculation treatment has been applied to an AMD sample using 5 g clay (bentonite), 20, 30, 40, 50 and 60 mL of 0.10 M Al^{3+} in $AlCl_3$ and 0.10 M Mg^{2+} in $Mg(OH)_2$ dosages respectively. The pH, conductivity, turbidity, zeta potential and dissolved oxygen (DO) of the samples were measured before and 1 hour after treatment. A one litre AMD sample was poured into a litre glass beaker, 5.0 g of clay added to the sample and mixed in a flocculator at 250 rpm for 2 minutes and reduced to 100 rpm for 10 minutes. The sample was allowed to settle for 1 hour after which 200 mL of the supernatant was poured into five 500 mL glass beakers. Dosages of 20, 30, 40, 50 and 60 mL af-PACl synthetic polymer were added to the samples using 100 mL plastic syringes respectively. The samples settled for 1 hour, and then the pH, conductivity, turbidity, zeta potential and DO were measured. A similar set of experiments was conducted using a synthetic polymer made of a mixture of 5.0 g clay, 0.10 M Al^{3+} in $AlCl_3$ and 0.10 M Mg^{2+} in $Mg(OH)_2$. Similar measurements were conducted before and after 1 hour settling from a jar test.

2.1 AMD sampling

The samples were collected from the Western Decant in Krugersdorp in a 25 litres plastic drum.
The sample was air-tied and stored at room temperature. The pH, conductivity, turbidity, ORP and DO of the AMD sample before mixing were 2.08, 4.94 mS/cm, 105 NTU, 234 mV and 4.5 mg/L respectively.

2.2 Coagulants

Inorganic coagulants of 0.10 M of $Al^{3+}$and Mg^{2+} ions (a concentration obtained from the literature) were dosed for coagulation-flocculation of the AMD.

The calculation of the mass of metal salt to obtain 0.10 M of M^{n+} (M^{n+} = *Al or Mg*) was as follows:
Monoprotic metal salts (MCl_3)

0.10 M of M^{3+} x *mass of* $M^*Cl_3 6H_2O$ (M^*= *Al*) (9)

0.10 M of Mg^{2+} *x mass of* $M^*(OH)_2$ (*M = Mg*) (10)

Table 1 shows the monoprotic metal salts dosed into the AMD samples.

Table 1 here

2.3 Procedure in jar tests.

The equipment used for the jar tests was a *BIBBY Stuart Scientific Flocculator (SW1 model)*, which has six adjustable paddles with rotating speeds between 0–350 rpm. A 200 mL sample of AMD containing 6.3 g of solid particles was poured into each of the five 500 mL glass beakers for the test. Rapid mixing was set at 250 rpm for 2 minutes, followed by slow mixing at 100 rpm for 10 minutes, a normal standard recommended in a jar test.

3.0 Experiments

3.1 Experiment (A): Jar test with clay and af-PACl polymer dosed separately

The pH, conductivity, turbidity, zeta potential and DO of the sample were measured. Five 500 mL glass beakers were filled with 200 mL samples of AMD with parameters mentioned under sub-section 2.1. A 1.2 L of AMD sample was dosed with 5 g pulverized clay and treated in a jar test at 250 rpm for 2 minutes and reduced to 100 rpm for 10 minutes. The sample was allowed to settle for 1 hour after which 200 mL of the supernatant was poured into five 500 mL glass beakers. The samples were dosed with 20, 30, 40, 50 and 60 mL of 0.10 M af-PACl synthetic polymer of $Mg(OH)_2$. The samples were allowed to settle for 1 hour, after which the measurements were conducted.

3.2 Experiment (B): Jar test with a polymer of clay and af-PACl polymer dosage

A similar set of experiments, where 5 g of clay was mixed with 0.10 M Al^{3+} in $AlCl_3$ and 0.10 M of Mg^{2+} in $Mg(OH)_2$ to produce a synthetic polymer, was used. A 200 mL of AMD sample was poured into five 500 mL glass beakers, treated in a jar test at 250 rpm for 2 minutes and reduced to 100 rpm for 10 minutes. The samples settled for 1 hour after which similar measurements were conducted.

3.3 Performance evaluation

The pH was used as a determinant to assess the rate of hydrolysis and hydrolytic potential of the coagulants (Al^{3+} and Mg^{2+} salts) at different mixing duration, whereas the concentration and turbidity were measured to determine the ionic potential and removal of colloidal particles from the samples respectively.

3.3.1 pH measurement

A SensoDirect Multimeter (*made in South Africa*) pH/ORP/DO/CD/TDS meter with an electrode filled with silver chloride solution and the outer glass casing with a small membrane covering at the tip was used. The equipment was calibrated with standard solutions with pH of 4.0 and 7.0 before use.

3.3.2 Conductivity

A similar Multimeter instrument as described in sub-section 3.3.1 was used. The CD probe was connected and the measurement was selected using the appropriate button, and the CD reading was displayed.

3.3.3 Dissolved oxygen

A similar Multimeter instrument as described in sub-section 3.3.1 was used. The DO probe was connected and the measurement was selected using the appropriate button, and the DO reading was displayed.

3.3.4 Oxidation reduction potential

A similar Multimeter instrument as mentioned in sub-section 3.3.1 was used. The ORP probe was connected and the measurement was selected using the appropriate button, and the ORP reading was displayed.

3.3.6 Turbidity measurement

A Merck Turbiquant 3000T Turbidimeter (*made in Japan*) was used to determine turbidity or the suspended particles in the supernatant, using NTU as a unit of measure. It was calibrated with 0.10, 10, 100, 1000 and 10000 NTU standard solutions.

4.0 RESULTS

Fig. 1 shows the diagram of an aqueous colloid with ions in the double and stern layers.
Fig. 1 here
Figs. 2 and 3 represent the % E, DO and ORP in AMD sample dosed with 5 g/L clay, 0.1 M $AlCl_3$ and 0.1 M $Mg(OH)_2$, when the clay dosage was conducted in a jar test and the supernatant was dosed with a polymer of $AlCl_3$ and $Mg(OH)_2$, whereas in the other set of experiments, the AMD sample was dosed with a polymer of the three reagents.

Fig. 2 here

Fig. 3 here

Figs. 4 and 5 represent the pH, DO and ORP in the AMD sample of the two sets of experiments as conducted in the results shown in Figs. 2 and 3.

Fig. 4 here

Fig. 5 here

Figs. 6 and 7 represent the ORP vs pH in AMD sample of the two sets of experiments as conducted in the results shown in Figs. 2 and 3.

Fig. 6 here

Fig. 7 here

Figs. 8 and 9 represent the % E vs ORP in AMD sample of the two sets of experiments as conducted in the results shown in Figs. 2 and 3.

Fig. 8 here

Fig. 9 here

Fig. 10 represents the SEM images of the AMD samples dosed with clay, $AlCl_3$ and $Mg(OH)_2$.

Fig. 10 here

Table 2 here

4.0 DISCUSSION

The main objective in this study is the investigation of the micro-and macro-chemical reactions which cause the destabilization-hydrolysis reaction. This will then make it easier to elucidate on the physico-chemical interactions occurring during the coagulation-flocculation process, a precursor to nucleation, crystallization and sedimentation/settling; a chain reaction which is still unclear in wastewater treatment. The studies which have been conducted are mainly to investigate the best technologies and reagents (coagulants/flocculants/aids) to be employed in wastewater treatment, an approach not contemplated in this study. In this study the focus is on the physico-chemical strength mechanisms of the respective reagents (af-polymers) to effectively destabilize the double layer of the aqueous colloids, thereby weakening the repulsive forces and promote agglomeration. In a normal coagulation-flocculation process with coagulant/flocculent, (counter ionic to the charges of the colloids) the volume of the diffuse layer which maintains electro-neutrality is lowered, the thickness of the diffuse layer is reduced and the van der Waals force becomes predominant, causing the net force to become attractive. The effectiveness of the process determines the rate of agglomeration and adsorption (turbidity removal).

The turbidity removal efficiency (Fig. 2) in the AMD sample in experiment (A) is relatively high, in a range of 97.2-99.8 %. This is a phenomenal turbidity removal but an explanation can still be derived from the slight difference obtained between the dosages (20-60 mL). The experimental results (Fig. 2) indicate that for the 30, 40 and 60 mL dosages, the best removal efficiencies were obtained. The ORP is reduced from 232 mV (untreated AMD) to values in the range of 145-193 mV (reduced to a range of 62.5-83.1 %), and also showed a correlation with the turbidity removal efficiency. That is shown by the AMD samples with 30, 40 and 60 mL dosage, showing slightly higher removal efficiencies (Fig. 2). In general, the ORP values exhibit a constant changing trend with increasing dosage. The DO changed from 4.5 mg/L (untreated AMD) to a range of 4.0-7.1, the AMD samples with 20, 40 and 50 mL dosage showing values which are lower (reduction occurred and dropped to 0.41, 0.20 and 0.5 mg/L respectively) than for the untreated AMD sample. This indicates that some oxygen molecules have been consumed during the destabilization-hydrolysis process, the behaviour which was not shown by the AMD sample with 30 and 60 mL dosage (oxidation occurred and increased by 3.5 and 3.6 mg/L respectively). It is not easy to explain the oxidation mechanisms relating to the respective dosages as they are both on either side of the intermediate dosage of 40 mg/L.

The strength of the reagent can arbitrarily be explained by the ability to weaken the electrostatic forces of the aqua-colloid (Fig. 1) and allow the van der Waals forces of attraction to induce collision-vibration between neighbouring aqua-colloids, a phenomenon which results in the agglomeration with the aid of the reagent (af-PACl). This occurs due to the screening effect of the electrostatic repulsive forces between the charged particles in solution and that promotes the rate of particle flocculation through

short-range van der Waals interactions. On the other hand, the screening effects reduce the electro-attractive interactions between the charged flocculants and the oppositely charged particles, thus strongly affecting the flocculation rate and polymer efficiency (Fig. 1). The presence of the polymer is also expected to play a role on the flocculent conformations by promoting gel formation, flocculent folding and collapse, which leads to optimal agglomeration. This reaction occurs during the destabilization on the aqua-colloids, a determining process of the effectiveness of the turbidity removal (Ntwampe *et al.*, 2015). The efficiency of the af-PACl polymer exhibited by the experimental results in this study, can be explain by the hydrolysis of both metal ions (Al^{3+} and Mg^{2+}) after being added to the AMD sample. Eqs. 3-7 show that the reactivity of the coagulant/flocculent is influenced by physico-chemical properties, such as the charge on the particle, thickness of the layer surrounding the shear plane, dielectric constant of liquid, concentration and valence of the ions, charge of the electron and temperature.

The type of colloids, hydrophilic or hydrophobic, plays a pivotal role during the destabilization-hydrolysis-crystallization in wastewater treatment. The type of coagulant/flocculent is also essential and should be compatible to neutralize the electrostatic repulsive forces which keep the colloids apart. This has been confirmed by the work conducted by Libecki *et al.*, (2008) where it was stated that the charge of molecules of colloids depends on the type and concentration of coagulating salt, as well as on the pH of the solution. Hydrophilic colloids have an affinity for water due to the existence of water soluble groups (e.g. amino, carboxyl, sulfonic, hydroxyl etc.) on the colloidal surface. These groups promote hydration and cause a water film to collect and surround the hydrophilic colloid, thus determining the rate of the destabilization-hydrolysis. Hydrophobic colloids have little affinity for water existence of water soluble detergents. They do not have any significant water film or water of hydration (e.g., clay, metal). Notwithstanding the fact that the empirical evidence of the reaction of $AlCl_3$ with $Mg(OH)_2$ remains unclear, it is suggested that the af-PACl polymer becomes denser after it is added to the solution which contains salts. The reaction between the reagents after addition to a colloidal suspension is shown by Eq. 11:

$$2\ AlCl_3 + 3\ Mg(OH)_2 \leftrightarrow 2\ Al(OH)_{3(s)} + 3\ MgCl_{2(aq)} \quad (11)$$

$$MgCl_{2(aq)} + 2\ H_2O \leftrightarrow Mg(OH)_{2(s)} + 2\ HCl_{(aq)} \quad (12)$$

The $Mg(OH)_{2(aq)}$ (Eq. 11) is actually in the form of $Mg^{2+}{}_{(aq)}$ and $OH^{-}{}_{(aq)}$, where Mg^{2+} ions dissolve in the AMD solution and hydrolyse to form $Mg(OH)_{2(s)}$ precipitates (Eq. 12), which react with $Al(OH)_{3(s)}$ to form an acid-free polymer. These chemical reactions indicate that the af-PACl polymer of $Mg(OH)_2$ behaves partially as a coagulant due to the presence of the cationic Al^{3+} and Mg^{2+} ions. This is a very cost effective polymer, which doesn't require a sophisticated production process that includes a special reactor and restricted operating conditions. As Eq. 11 showed that there is double hydrolysis taking place, the effective turbidity removal (Figs. 2 and 3) confirms that the destabilization-hydrolysis with an af-PACl polymer is attributed to both Al^{3+} and Mg^{2+} ions in a polymer. The turbidity results also predict that charge neutralization, enmeshment in a precipitate and adsorption and inter-particle bridging are the predominant reactions during destabilization.

The turbidity results (Fig. 3) in AMD samples with a polymer of 5 g clay, 0.1 M $FeCl_3$ and 0.1 $Mg(OH)_2$ in experiment (B) showed a similar removal efficiency compared to the results shown in experiment (A), Fig. 2. It is only in the sample with 40 mL dosage that the turbidity removal is slightly lower (94.8 %), whereas it is in a range of 97.9-99.3 % in the other dosages. In view of the fact that the drop is so insignificant, it cannot be clearly elucidated because it occurred in a sample with intermediate dosage (between the lowest and the highest dosages). It has to be taken into account that the effectiveness of the polymer interaction in solution, or at the solid-liquid interface, depends on the nature of the polymer(s) and solid surface, solution chemistry, and the interaction, can profoundly change the charge properties of polymers and more vitally the conformation of polymers, both of which are ascertained to be main controlling factors in flocculation with polymeric flocculants. This has also been confirmed in the study by Somasundaran *et al.*, (1989) using two polymers to treat an alumina suspension where the dual polymer is effective and can enhance flocculation at lower dosages. The presence of the clay content is an attribute to the effectiveness of the polymer (af-PACl). The advantage in the utilization of clays (bentonite) is that they mostly have a net charge on their surface (usually negative). This surface charge arises from isomorphous substitutions, lattice imperfections and the broken or unsatisfied bonds that arise from the large surface area that characterizes these clay minerals. These surface charges (coupled with the clay minerals' large surface areas) allow the clay

minerals to adsorb ions (usually cations) to their surface (Figs. 2 and 3). This allows the clay minerals to act like a catalyst for many chemical reactions, and to exchange ions with their surroundings. The clay minerals also have the ability to adsorb the H^+ (cationic exchange capacity) onto their surface, resulting in the neutralization of the charge (Lorenz, 1969).

The conductivity values obtained in the two set of experiments of the AMD sample in experiment (A), range between 4.55-5.44 mS/cm, and that in the sample in experiment (B), range between 4.91-5.79 mS/cm and show a significant change (Figs. 4 and 5). The conductivity in the AMD samples of the former is lower than that in their corresponding AMD samples of the latter experiment. The conductivity in the samples dosed with 20 and 30 mL (4.55 and 4.84 mS/cm respectively) of experiment (A) and the 20 mL dosage (4.91 mS/cm) of experiment (B) is slightly less than that of the untreated AMD sample (4.94 mS/cm). This indicates that dissolved cations (Mg^{2+}) and the conjugate base (Cl^-) of the polymer reacted after dosing (destabilization-hydrolysis) as it has been stated previously that the Mg^{2+} hydrolysed and forms monomers, which bridged with $Al(OH)_3$ to polymerize. On the contrary, the AMD samples with 40-60 mL of experiment (A) and 30-60 mL dosage of experiment (B) are higher than that of untreated AMD sample. It is suggested that the high conductivity is caused by the Cl^- ions with Mg^{2+} converted into monomers (hydrolysis), enhancing the turbidity removal (Figs. 2 and 3).

The differential pH values between the untreated AMD sample (2.08) and the treated AMD sample of experiment (A) decreased with increasing dosage in a range of 2.86-3.79, whereas the pH in the AMD samples of experiment (B) increased in a range of 2.54-3.68. The decreasing and increasing trends of the pH in experiments (A) and (B) respectively is attributed to the clay mineral, because it is the only reagent changing the dosing used [dosed alone as reagent-experiment (A), and dosed as a polymer with $FeCl_3$ and $Mg(OH)_2$-experiment (B)]. The inference to this is that the clay minerals have the ability to adsorb the (H^+) ions in the solution, the chemistry of its adsorption potential behaved differently when added alone, compared to when added as a polymer (Lorenz, 1969). The chemical reactivity turned the pH to be inversely proportional to increasing dosage (experiment A) and directly proportional to increasing dosage (experiment B). The correlation between the pH changing patterns in experiments (A) and (B) confirms that the clay-$FeCl_3$-$Mg(OH)_2$ reacted with the AMD sample in a form of a polymer, using "sweep flocculation" as a predominant adsorption mechanism as stated by Peavy (1985) and Zhang *et al*., (2006). Experiment (A) is in agreement with the finding by Ntwampe *et al*., (2013) that the rate of hydrolysis is determined by the decreasing trend of the pH in the solution. Experiment (B) revealed that the reactivity of the clay mineral can alter the correlation between the pH changing trend and the turbidity removal (Figs. 2 and 3). It is postulated that the clay mineral adsorbed more protons with increasing rate of hydrolysis, which occurs with increasing dosage (adsorption of protons is directly proportional to the concentration of dosage). This postulate applies when the clay minerals react with the AMD sample in a polymeric form. Although the clay affected the changing behaviour of the pH (experiments A and B), it didn't interfere with the turbidity removal efficiency of the polymer (94.8-99.9 %).

The ORP was reduced from 234 mV in the untreated AMD sample to a decreasing trend in a range of 193-146 mV in the sample of experiment (A). The ORP values showed an insignificant decreasing trend with increasing dosage, showing a difference in a range of 41-88 mV in comparison with the untreated AMD sample. The ORP values in the AMD samples of experiment (B) showed a slightly higher decreasing trend compared to those in their corresponding samples of experiment (A), in a range of 212-151 mV. This indicates that the samples of experiment (B) have a higher capacity to either release or accept electrons from chemical reactions compared to experiment (A). The addition of the polymer reduced the capacity of the samples in both experiments (A) and (B) to either accept or release the electrons, which indicates that the oxidation reaction occurred during the chemical reactions. The relationship between the pH and the ORP is such that the more basic (release of OH^-) of the samples, the less redox potential (releasing or accepting of electrons) the samples acquired.

The DO showed an inconsistent changing trend from 4.5 mg/L in the untreated AMD sample to a range of 4.0-7.1 mg/L (experiment A), and 4.0-5.3 mg/L (experiment B). The samples with 20, 40 and 50 mL dosage (experiment A) yielded similarly equal DO values (4.1, 4.3 and 4.0 mg/L respectively), whereas the samples with 30 and 60 mL dosage also yielded higher/equal values (7.0 and 7.1 mg/L) respectively, whereas the AMD samples with 20, 40, 50 and 60 mL dosage (experiment B) showed slightly lower and similarly equal DO values (4.4, 4.5, 4.1 and 4.0 mg/L respectively), and only the sample with 30 mL yielded a slightly higher value (5.3 mg/L). This observation indicates that there is ingress or release of O_2 during hydrolysis-nucleation-adsorption.

In Fig. 6 the correlation between the pH and ORP in AMD sample in experiment (A) is shown. The correlation coefficient of the two parameters is 99.8 %.

In Fig. 7 the correlation between the pH and ORP in AMD sample in experiment (B) is shown. The correlation coefficient of the two parameters is 99.8 %.

In Fig. 8 the correlation between the % E and ORP in AMD sample in experiment (A) is shown. The correlation coefficient of the two parameters is 87.0 %.

In Fig. 9 the correlation between the % E and ORP in AMD sample in experiment (B) is shown. The correlation coefficient of the two parameters is 73.7 %.

In Fig. 10 the SEM images of the AMD sludge of the sample in experiment (A) and the SEM images of the AMD sludge in experiment (B) at a magnification of 2500x is shown.

The SEM micrographs show flocculent branching which plays a key role since it is largely controlling the polymer interaction behaviour with the particles. It is suggested that the branching induces important differences in the floc structure, compactness, and fractal dimensions, which affect the sedimentation rates and floc strength. The potential impact of the solution ionic strength is due to the presence of dissolved ions of a multivalent electrolyte (Al^{3+} and Mg^{2+} salts) in the solution also plays a pivotal role. The SEM micrograph 10A is the AMD sludge in experiment (A) showing dense and small flocs located apart, dense on the left and small on the right, with very few cavities. The SEM micrograph 10B represents the AMD sludge in experiment (B), where there are dense flocs distributed throughout the slide with a limited number of cavities. The two micrographs show a sponge-cake like structure linked together, showing adsorption efficiency of more than 85 %. The cavities showed that they are sealed as going downward, showing no or insignificant amount of turbid materials which can pass through the adsorbate.
In Table 2 the comparison of the pH, conductivity, turbidity, DO and ORP in 5 g/L clay and the untreated AMD sample is shown.

The Pearson correlation coefficient (r) is used to calculate the relation between pH and residual turbidity, using Eq. 13.

$$r = \frac{n(\Sigma xy)-(\Sigma x)(\Sigma y)}{\sqrt{[n\Sigma x^2-(\Sigma x)^2][n\Sigma y^2-(\Sigma y)^2)]}} \qquad (13)$$

According to the correlation coefficient, (0.70 or higher is very strong relationship), (0.40-0.69 is a strong relationship), and (0.30-0.39 is moderate relationship). The parameters obtained for the ORP and pH of the AMD sample in experiment (A) or the AMD sample in experiment (B), (Figs. 6 and 7) are:

$\Sigma x_{exp(A)} = 18.1$, $\Sigma x^2_{exp(A)} = 65.9$, $\Sigma y_{exp(A)} = 7.7$, $\Sigma y^2_{exp(A)} = 11.9$ and $\Sigma xy_{exp(A)} = 27.5$

$\Sigma x_{exp(B)} = 16.2$, $\Sigma x^2_{exp(B)} = 53.9$, $\Sigma y_{exp(B)} = 8.33$, $\Sigma y^2_{exp(B)} = 14.1$ and $\Sigma xy_{exp(B)} = 26.6$

The r-value obtained for the AMD samples (Fig. 6) in experiment (A) is 0.884 (88.4 %) with the range of the correlation coefficient from -1 to 1. The correlation coefficient for the samples thus falls within a range of strong relationship. This is validated by the R^2 of ORP vs pH of 0.9989 (99.9 %), as shown in Fig. 6. The r-value obtained for the AMD sample (Fig. 7) in experiment (B) is 991 (99.1 %) and thus also has a strong relationship. This is validated by the R^2 of ORP vs pH of 0.9976 (99.8 %), as shown in Fig. 6.

5.0 CONCLUSION

The efficiency of the af-PACl polymer exhibited by the experimental results obtained in this study can be explained by the hydrolysis of both metal ions (Al^{3+} and Mg^{2+}) after being added to the AMD sample. The results showed that the addition of the clay to the AMD sample as a reagent (A) or a polymeric component (B) does not affect the turbidity removal, but the rate of hydrolysis (pH changing pattern) and ORP. The experimental results showed that there is a correlation between the ORP and the pH, and also showed that oxidation takes place during the destabilization-hydrolysis process. The results also showed that the conductivity plays a role during the destabilization-hydrolysis process, (correlation between changing rate of the conductivity and the turbidity). The DO observation results of experiments (A) and (B) showed that there is an ingress or release of O_2 during hydrolysis-nucleation-adsorption.

Acknowledgements: This work is based on the research financially supported by the South African Research Chairs Initiative of the Department of Science and Technology and National Research Foundation of South Africa (Chair Grant No.: 86880, UID 85643, Grant No.: 85632). Any opinion, finding or conclusion or recommendation expressed in this material is that of the author(s) and the NRF does not accept any liability in this regard.

REFERENCES

1) Aboulhassan, M.A. Souabi, S. Yaacoubi, A. and Baudu, M., 2006. Removal of surfactant from industrial wastewaters by coagulation flocculation process, Interface Journal of Environmental Science & Technology, 3(4) 327-336.
2) Amuda, O.S, Amoo, A and Ajayi, O.O., 2006. Performance optimization of coagulant/flocculant in the treatment of wastewater from a beverage industry, Journal of Hazardous Material, 129. 69-72.
3) Ananikov, Valentin P.; Szilagyi, Robert; Morokuma, Keiji; Musaev, Djamaladdin G., 2005. "Can Steric Effects Induce the Mechanism Switch in the Rhodium-Catalyzed Imine Boration Reaction. A Density Functional and ONIOM Study". Organomet. 24, 8: 1938. doi:10.1021/om049156o.
4) Binnie, C. Kimber, M. and Smethurst, G., 2003. Basic Water Treatment, 3rd Ed, MPG Books, Bodmin, Great Britain.
5) Bolto, B. and Gregory, J., 2007. Organic polyelectrolytes in water treatment, Wat. Res. 41. 2301-2324.
6) Bratby, J., 2006. Coagulation and flocculation in water and wastewater treatment, 2nd ed., IWA Publishing, UK.
7) Burgess, J., De Jong, H.C. and Aguitar, Z.P., 2009, Biological Nanostructures, Materials, and Applications, vol. 16 (38) ECS Transaction, New Jersey.
8) Chang, Q. and Yu, M., 2004. An, application of macromolecular heavy metal flocculant in wastewater treatment, Chemosphere, 6, 42-47.
9) Cosgrove, T., 2005. Colloid science – Principles, methods and applications (Knovel ebook), Blackwell Publishing, UK.
10) Crittenden, J.C., Trussell, R.R., Hand, D.W., Howe, K.J. and Tchobanoglous, T. 2005.
11) Water treatment – Principles and design (2nd ed.) (Knovel ebook), John Wiley & Sons, USA.
12) Darekh, B.K. and Chen, Z., 2004, Miner. Metall. Proc. 4, 214-216.
13) Doymus, K., 2007, The Effect of Ionic Electrolytes and pH on the Zeta Potential of Fine Coal Particles, Turk. J. Chem. 31, 589-597.
14) Duan, J. and Gregory, J., 2002. Coagulation by hydrolysing metal salts, Elsevier B. V. UK.
15) Duan J. and Gregory J., 2003. Coagulation by hydrolyzing metal salts: Advances in Colloidal & Interface Science, 100-102. 475-502.
16) Edwards, A.C. and Withers, P.J.A., 2007. Linking phosphorus sources to impacts in different types of water body, Soil Use Manage, 23. 133-143.
17) Eikebrokk, B., 2007. Characteristics and treatability by coagulation. Comparison of Norwagian and Australian waters, Chemical water and wastewater treatment, IWA Publishing.
18) Fabris, R., Chow, C.W.K. Drikas, M. and Eikebrokk, B., 2008. Comparison of NOM character in selected Australian and Norwegian drinking waters, Wat. Res. 42. 4188–4196
19) Field, J.A., Kortekaas, S. and Lettinga, G., 1989. Thetann in theory of methanogenic toxicity,
20) Biol. Waste, 29. 241–262.
21) Freeze, S.D, Nozaic, D.J, Pryor, M.J, Rajogopaul, R, Trollip, D.L, Smith, R.A., 2001. Water Supply, vol. 1, IWA Publishing, SA.
22) Feng, W. and Nansheng, D., 2000. Photochemistry of hydrolytic iron (III) species and photo induced degradation of organic compounds. Chemosphere, 41. 1137-1147.
23) Firer, D., Friedler, E., Lahav, O., 2008. Control of sulfide in sewer systems by dosage
24) of iron salts: Comparison between theoretical and experimental results, and practical implications, Sci. Tot. Environ. 392. 145–156.
25) Gallato, S.L., Peterson, M., Alexandre, N.Z., da Costa, J.A.D., Izidoro, G., Sorato, L., Levati, M., 2009, Incorporacao de residuo do tratamento de drenagem acida em massa de ceramic a vermelha, Ceramica, 55, 53-60.
26) Geldenhuys, A.J., Maree, J.P., Fourie, W.J., Smit, J.J., Bladergroen, B.J. and Tjati, M., 2001. Acid mine drainage treated electrolytically for recovery of hydrogen, iron(II) oxidation and sulphur production, Submission at the 8th International Congress on Mine Water & Environment in Johannesburg, South Africa
27) Ghaly, A.E. Snow, A. Faber, B.E., 2006. Treatment of grease filter washwater by chemical coagulation. Canadian Biosystem Engineering, 48.13-6.22.
28) Goldberg, S., 2002. Competitive Adsorption of Arsenate and Arsenite on Oxides and Clay Minerals, Soil Science Society of America, 66. 413-421.
29) Gupta, R., 2007, Advanced Coal Characterization: A Review. Energy & Fuels, 21, 451-460.
30) Kleijn, W.B. and Ostzr, J.D., 1982, A model of swelling and tactoid formation, Clay and Clay Min. 30 (5) 383-390.
31) Kosmulski M. and Saneluta C., 2004. Point of zero charge/isoelectric point of exotic oxides: Tl_2O_3', J. Colloid and Interf. Sci. 280 (2) 544-545.
32) Haselberg, Rob; van der Sneppen, Lineke; Ariese, Freek; Ubachs, Wim; Gooijer, Cees; de Jong, Gerhardus J.; Somsen, Govert W., 2009. "Effectiveness of charged non-covalent polymer coatings against protein adsorption to silica surfaces studied by evanescent-wave cavity ring-down spectroscopy and capillary electrophoresis". Anal. Chem. 81(24) 10172–10178.
33) Herrera, P.S., Uchiyama, H., Igarashi, T., Asakura, K., Ochi, Y., Ishizuka, F., Kawada, S., 2007, Acid mine drainage treatment through a two-step neutralization ferrite-formation process in northern Japan: Physical and chemical characterization of the sludge, Mineral Eng. 20, 1309-1314.
34) Hower, J., Graham, U.M., Dozier, A., Tseng, M.T. and Khatri, R.A., 2008, Association of the sites of heavy metals with nanoscale carbon in a kentucky electrostatic precipitator fly ash, Environ. Sci. and Technol. 42, 8371-8477.
35) Huang, X., Finkelman, R.B., 2008, Understand th Chemical Properties of Macerals and Minerals in Coal and its Potential Application for Occupational Lung Disease Prevention. J. Toxicl. Environ. Health, Part B, 11, 45-67.
36) Kemmer, J., 1988, Nalco Water Handbook. 2nd edition. McGraw-Hill, New York.
37) Khanal, S. K. and Huang, J. C., 2003, "ORP-based oxygenation for sulfide control in anaerobic treatment of high-sulfate wastewater." Wat. Res. 37, 2053-2062.
38) Khanal, S. K. and Huang, J. C., 2006, "Online oxygen control for sulfide oxidation in anaerobic treatment of high-sulfate wastewater." Wat. Environ. Res. 78 (4) 397-408.
39) Kishida, N., Kim, J. H., Chen, M., Sasaki, H. and Sudo, R., 2003, "Effectiveness of oxidation-reduction potential and pH as monitoring and control parameters for nitrogen removal in swine
40) wastewater treatment by sequencing batch reactors." J. of Biosci. and Bioeng. 96, 285-290.
41) Kosmulski M. and Saneluta C., 2004, Point of zero charge/isoelectric point of exotic oxides: Tl2O3', J. Colloid and Interf. Sci. 280(2) 544-545.
42) Kurniawan, T.A. Chan, W.S., Lo W-S. and Babel, S., 2006. Chemical Engineering, 118. 83–87.
43) Labeschagne, C., 2005. Investigation of the acid mine drainage potential on the Kopanong rock dump, Vaal Reefs, A dissertation submitted for MSc degree at North West University, RSA.
44) Lee, J., 2001. Application of liquid electron theory to the cross effect between ionic and electric charge flow in semiconduct oxide. Journal Physics and Chemistry of Solids, 62. 1263-1270.
45) Libecki, B. and Dziejowski, J., 2008, Optimization of Humic Acids Coagulation with Aluminum and Iron(III) Salts, Polish J. of Environ. Stud. 17, 397-403
46) Lorenz, P.B., 1969, Surface conductance and electrokinetic properties of kaolinite beds, Clays and Clay Min. 17, 223-231.

47) Meghzili B., 2008. Tests of Coagulation - Flocculation by Aluminum Sulphate and Polycations Al on Raw Waters of the Station of Treatment Skikda (Algeria): European J. Sci. Res. 23(2): 268-277.
48) Maree, J.P., 2004, Treatment of industrial effluent for neutralization and sulphate removal, A thesis submitted for PhD at the North West University, RSA.
49) Metcalf, W and Eddy, C., 2003. Wastewater Engineering. 4th. McGraw-Hill Inc, New York.
50) Molony, J., 2005. Colour coating & corrosion SA-J. for OCCA SA, SAPMA. Leaf Media. Natal (SA).
51) Naicker, K., Cukrowska, E., & McCarthy, T.S. 2003. Acid mine drainage from gold mining activities in Johannesburg, South Africa and environs, Environ. Pol. 122, 29-40.
52) Neto, M. A. S., Villwock, R., Scheer, S., Steiner, M. T. A., & Dyminski, A. S., 2010, Visual data mining techniques applied for the analysis of data collected at itaipu power plant, Técnicas de Mineração Visual de Dados aplicadas aos dados deinstrument.
53) Nielsen, A.H., Lens, P., Vollertsen, J. and Hvitved-Jacobsen, T., 2005. Sulfide-iron interactions in domestic wastewater from a gravity sewer, Water Res. 39. 2747–2755.
54) Nielsen, A.H., Vollertsen, J., Jensen, H.S., Wium-Andersen, T. and Hvitved-Jacobsen, T., 2008. Influence of pipe material and surfaces on sulfide related odor and corrosion in sewers, Wat. Res. 42. 4206–4214.
55) Nielsen, A.H., Hvitved-Jacobsen, T. and Vollertsen, J., 2008. Effects of pH and Iron Concentrations on Sulfide Precipitation in Wastewater Collection Systems, Water Environ. Res. 80. 380–380.
56) Ntwampe, I.O. Jewell, L.L. Hildebrandt, D and Glasser, D., 2013. The effect of mixing on the treatment of paint wastewater with Fe^{3+} and Al^{3+} salts, Journal of Environmental Chemistry and Ecotoxicology, 5(1) 7-16.
57) Ntwampe, I.O., Waanders, F., Fosso-Kankeu, E and Bunt, J., Reaction Dynamics of Iron and Aluminium Salts Dosage in AMD Using Shaking As an Alternative Technique in the Destabilization-hydrolysis Process, Intern. Sci. Res. J. accepted on the 17 June 2015.
58) Parra-Barraza, H., Hernandez-Montiel, D., Lizardi, J. Hernandez, J. Urbina, R.H. and Valdez, M.A., 2003, Fuel 82, 869-874.
59) Petrik, L.F., White, R.A., Klink, M.J., Somerset, V.S., Burgers, C.L. and Fey, M.V., 2003. Utilization of South African Fly Ash to Treat Acid Coal Mine Drainage, and Production of High
60) Quality Zeolites from the Residual Solids, Submission of International Ash Utilization Symposium, October 20-22, 2003, Lexington, Kentucky, USA
61) Pratt, C., Shilton, A., Pratt, S., Haverkamp, R.G. and Elmetri, I., 2007. Effects of redox potential and pH changes on phosphorus retention by melter slag filters treating wastewater, Environmental Science and Technology, 4 (18), 6583-6590.
62) Sabah, E. and Erkan, Z.E., 2006, Fuel, 85, 350-359.
63) Santos, J.A., Nunes, L.A.PL., Melo, W.J. and Araujo, A.S.F., 2011, Tannery sludge compost amendment rates on soil microbial biomass of two different soils. Euro. J. of Soil Biol. 47, 146-151.
64) Scholtz, F. 2010, (Ed.), Electroanalytical Methods, 2nd ed., Springer-Verlag, Germany, pp. 3–9.
65) Semerjian, L. and Ayoub, G.M., 2003, High-pH-magnesium coagulation-flocculation in wastewater treatment, Adv. in Environ. Res. 7, 389-403.
66) Sibrell, P. L. Montgomery, G.A., Ritenour, K.L., and Tucker, T.W. 2009. Removal of
67) phosphorus from agricultural wastewaters using adsorption media prepared from acid mine drainage sludge. Water Research, 43(8) 2240-2250.
68) Silva, L.F.O., Monero, T. and Querol, X., 2009a, An introductory TEM study of Fe-nanominerals within coal fly ash, Sci. of Environ. 407, 4972-4974.
69) Silva, L.F.O., Macias, F., Oliviera, M.L.S., Da Boit, K.M. and Waanders, F., 2010a, Leaching of potential hazardous elements of coal cleaning rejects, Environ. Monitor. and Assess. DOI:10. 1007/s10661-010-1340-8.
70) Sincero, A.P. and Sincero, G.A., 2003. Physical-chemical treatment of water and wastewater, IWA Publishing, Londao, USA.
71) Skalny, J., Marchand, J. and OdJer, I., 2001. 'Sulfate attack of concrete',(E and FN Spon, London, UK.
72) Sharp, E.L., Parsons, S.A. and Jefferson, B., 2006. Seasonal variations in natural organic
73) matter and its impact on coagulation in water treatment, Sci. Tot. Environ. 363. 183–194.
74) Sharp, E.L., Jarvis, P., Parsons, S.A. and Jefferson, B, 2006. Impact of fractional character
75) on the coagulation of NOM, Colloids Surf. Physicochem. Eng. Aspects. 286. 104–111.
76) Sinha, P. ,Szilagyi, I.,Ruiz-Cabello, F.J.M.,Maroni ,P. and Borkovec, M. 2013. Attractive Forces between Charged Colloidal Particles Induced by Multivalent Ions Revealed by Confronting Aggregation and Direct Force Measurements, *J. Phys. Chem.* 4 (4) 648–652
77) Stoll, S, 2013, The Importance of Zeta Potential Measurements & Role of Ionic Strength in Flocculation Processes, Wat. Technol. 4 (1) 1-5
78) Somasundaran, P., Tjipangandjara, K. F., and Maltesh, C., (1989) in "Solid Liquid Separation: Waste Management and Productivity Enhancement" (H. S. Muralidhara, Ed.), p. 325. Battelle Press, Columbus, Ohio.
79) Sulkowski, W.W. Wolinska, A. Szoltysik, B. Bajdur, W.M. Sulkowska, A., 2005. Preparation and properties of flocculants derived from polystyrene waste. Elsier Ltd. Poland.
80) Suzuki, M., 1990. Adsorption Engineering, Kodansha Ltd, Japan.
81) Swartz, C.D. and Ralo, T., 2004. Guidelines for planning and design of small water treatment plants for rural communities with specific emphasis on sustainability and community involvement and participation, Silowa Printers, SA.
82) Syed Imran A., Shah, 1., Larry W., Kostiuk and Kresta, K.M., 2012, The Effects of Mixing, Reaction Rates, and Stoichiometry on Yield for Mixing Sensitive Reactions—Part I: Model Development, Intern. J. of Chem. Eng. Volume 2012 (2012), Article ID 750162, 16 pages
83) http://dx.doi.org/10.1155/2012/750162
84) Taylor, H.F.W., 1990. 'Cement chemistry', Academic Press Inc., San Diego, USA.
85) von Helmholtz, H.L.F and Abhandl, W, 1879. Physik. Tech. Reichsaslaldt, 1. 925.
86) Von Smoluchowski, M. , 1921. In "Graetz Handbuch der Electrizitiit und des Magnetismus"; VEB Georg
87) Wall, N.A. and Chopping, G. R. 2003. humic acids coagulation: influence of divalent cations. Appl. Geochem., 18. 1573.
88) Weber, W. J., Jr., 1972, Physicochemical Process for Water Quality Control, Wiley-Interscience, John Wiley & Sons, New York, pp. 61-109.
89) Wei, J., Gao, B., Yue, Q., Wang, Y., Li, W. and Zhu, X., 2009, Comparison of coagulation behaviour and floc structure characteristic of different polyferric-cationic polymer dual-coagulants in humic acid solution, Wat. Res. 43, 724–732.
90) Wei, J.C., Gao, B.W., Yue, Q.Y. and Wang, Y., 2010, Strength and regrowth properties of polyferric-polymer dual-coagulant flocs in surface water treatment, J. Haz. Mat. 175, 949–954.
91) Winfrey, B.K., Strosnider, W.H., Nairn, R.W. and Strevett, K.A., 2010, Highly effective reduction of faecal indicator bacteria counts in an ecologically-engineered municipal wastewater and acid mine drainage passive co-treatment system. Ecol. Eng. 36:1620–1626.

92) Widerska-Broz, M. and Rak, M., 2009. Effect of the type of aluminium coagulant and water pH on the destabilization of the colloid, Environ. Protect. Eng. 35. 63-72.
93) Wu, Y-M, Shi, C-F, Gu, J, Tan, Y, Wu, X L*, 2006. Microbial community structure in production water from a Daqing petroleum reservoir, Acta Pedologica Sinica,in press (in Chinese)
94) Zhang, Z.G., Luan, Z.K., Zhao, Y. Cui, J.H., Chen, .ZY. and Li, Y.Z., 2007, Breakage and regrowth of flocs coagulation with polyaluminum chloride (PACl)], Huan Jing Ke Xue. 28(2): 346-51.

Figures

Fig. 1: Double layer showing electrical charges (von Helmholtz et al., 1879).

Fig. 2: % E, DO and ORP in the AMD sample with added clay, followed by the af-AlCl polymer of $Mg(OH)_2$.

Fig. 3: % E, DO and ORP in the AMD sample with clay and af-AlCl polymer of $Mg(OH)_2$.

Fig. 4: pH, ORP, DO and conductivity in the AMD sample with clay, then af-AlCl polymer of $Mg(OH)_2$.

Fig. 5: pH, ORP, DO and conductivity in the AMD sample with clay and af-AlCl polymer of $Mg(OH)_2$.

Fig. 6: ORP vs pH in the AMD sample with clay and $AlCl_3$+$Mg(OH)_2$ polymer.

Fig. 7: ORP vs pH in the AMD sample with clay+$AlCl_3$+$Mg(OH)_2$ polymer.

Fig. 8: % E vs ORP in the AMD sample with clay and $AlCl_3$+$Mg(OH)_2$ polymer.

Fig. 9: % E vs ORP in the AMD sample with clay+$AlCl_3$+$Mg(OH)_2$ polymer.

Fig. 10: SEM micrographs of the AMD sample with clay, $AlCl_3$ and $Mg(OH)_2$ dosages.

Tables

Table 1: Metal salts and metal hydroxide dosed into the AMD sample.

Table 2: pH, conductivity, turbidity, DO and ORP in 5 g/L clay and untreated AMD sample.

Fig. 1

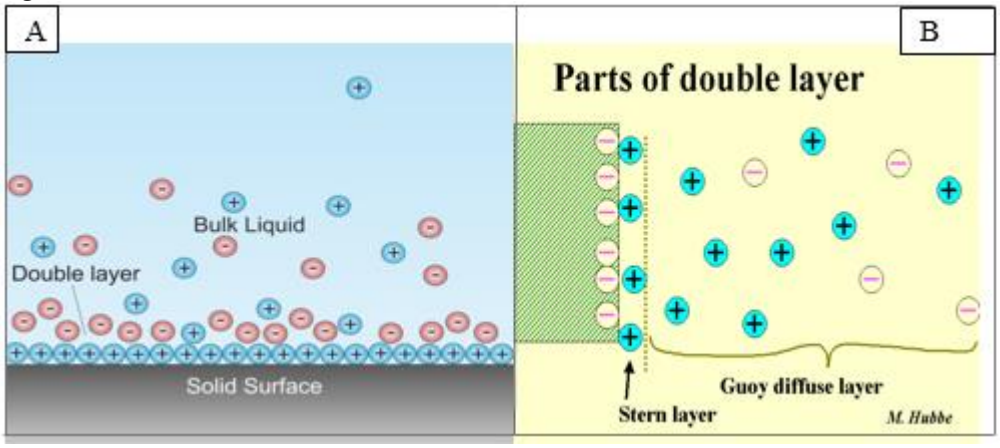

Fig. 2

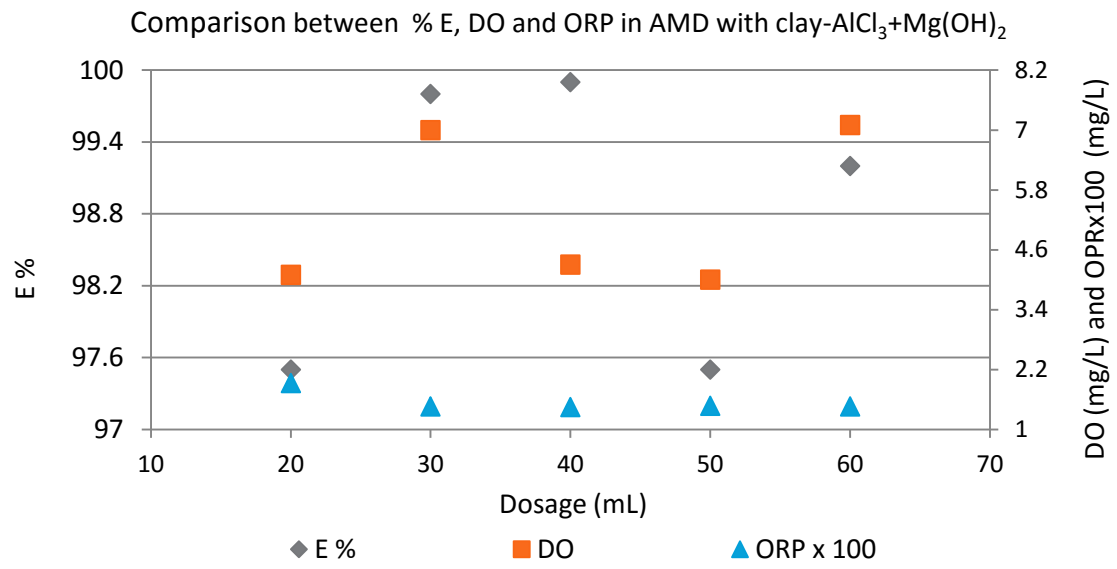
Comparison between % E, DO and ORP in AMD with clay-AlCl3+Mg(OH)2
100
99.4
98.8
98.2
97.6
97
E %
8.2
7
5.8
4.6
3.4
2.2
1
DO (mg/L) and OPRx100 (mg/L)
10
20
30
40
50
60
70
Dosage (mL)
E %
DO
ORP x 100

Fig. 3

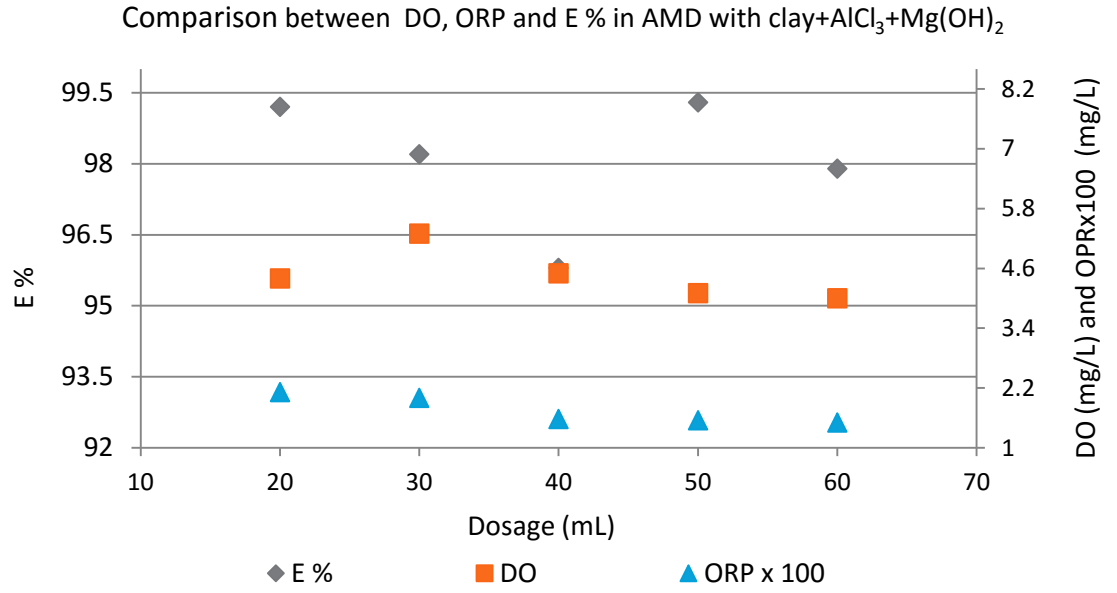
Comparison between DO, ORP and E % in AMD with clay+AlCl3+Mg(OH)2
99.5
98
96.5
95
93.5
92
E %
8.2
7
5.8
4.6
3.4
2.2
1
DO (mg/L) and OPRx100 (mg/L)
10
20
30
40
50
60
70
Dosage (mL)
E %
DO
ORP x 100

Fig. 4

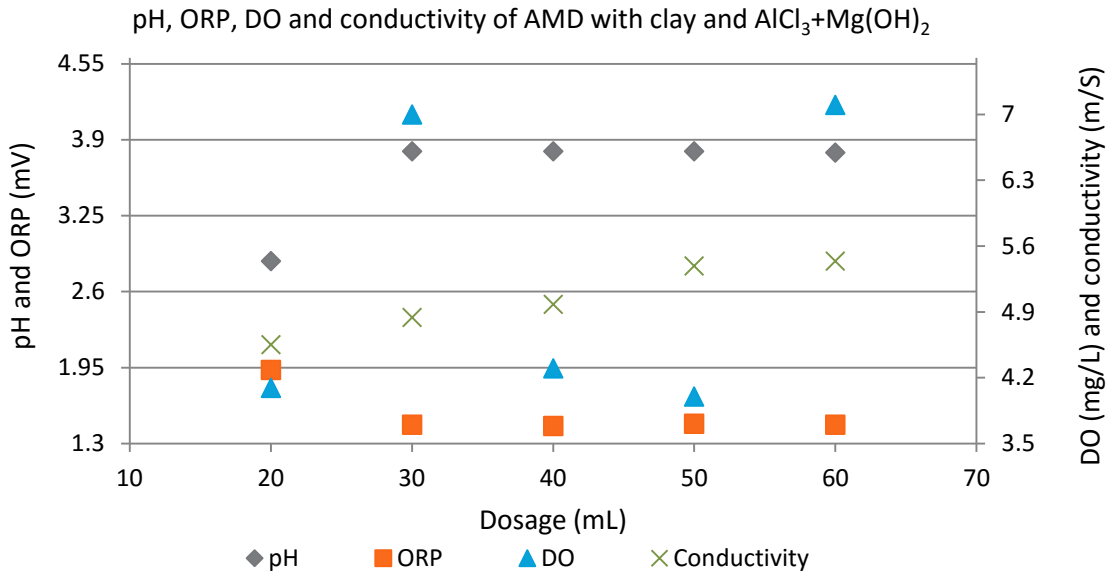

Fig. 5

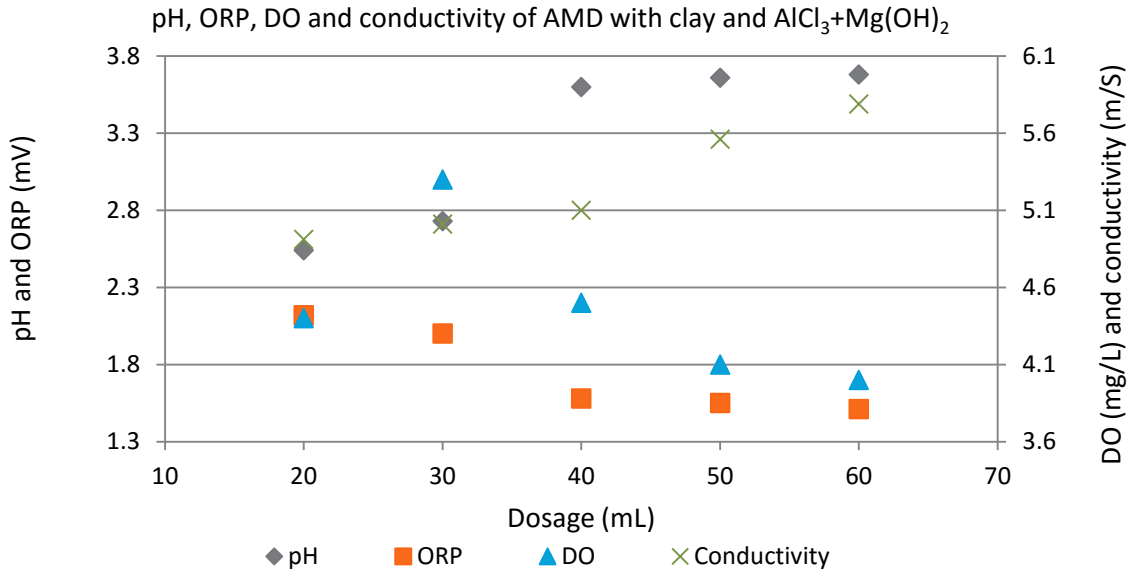

Fig. 6

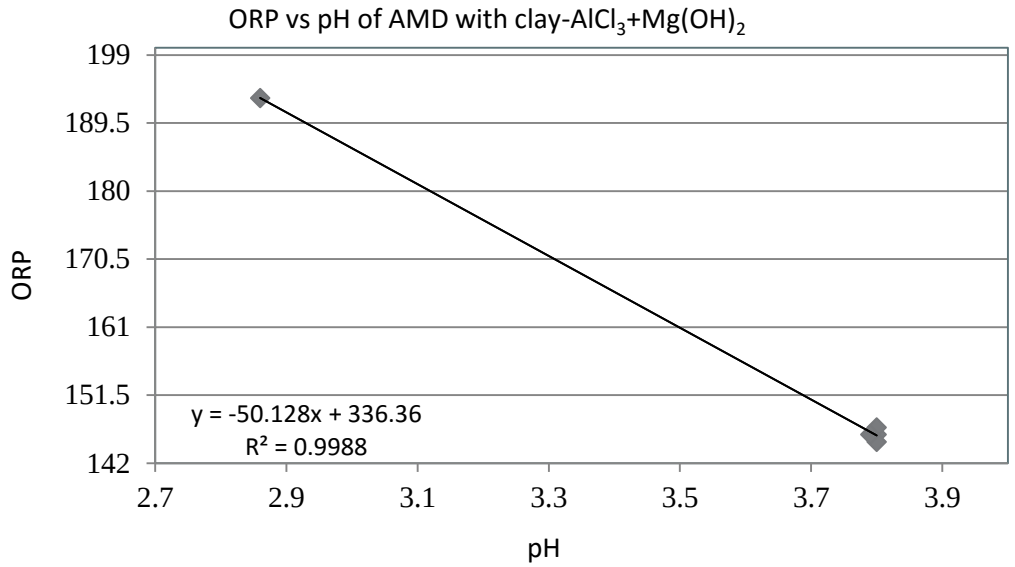
ORP vs pH of AMD with clay-AlCl3+Mg(OH)2
199
189.5
180
170.5
161
151.5
142
ORP
y = -50.128x + 336.36
R² = 0.9988
2.7
2.9
3.1
3.3
3.5
3.7
3.9
pH

Fig. 7

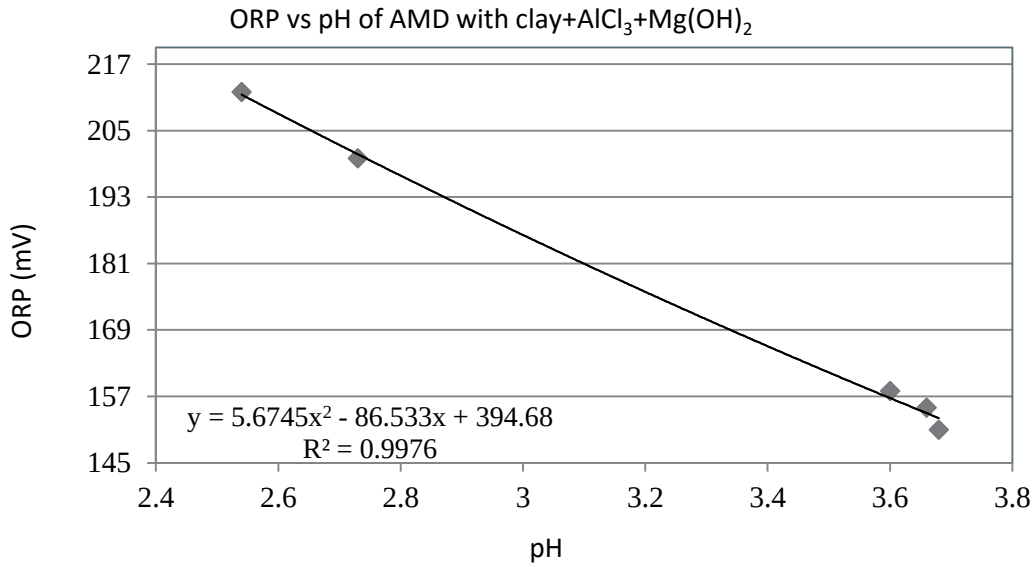
ORP vs pH of AMD with clay+AlCl3+Mg(OH)2
217
205
193
181
169
157
145
ORP (mV)
y = 5.6745x² - 86.533x + 394.68
R² = 0.9976
2.4
2.6
2.8
3
3.2
3.4
3.6
3.8
pH

Fig. 8

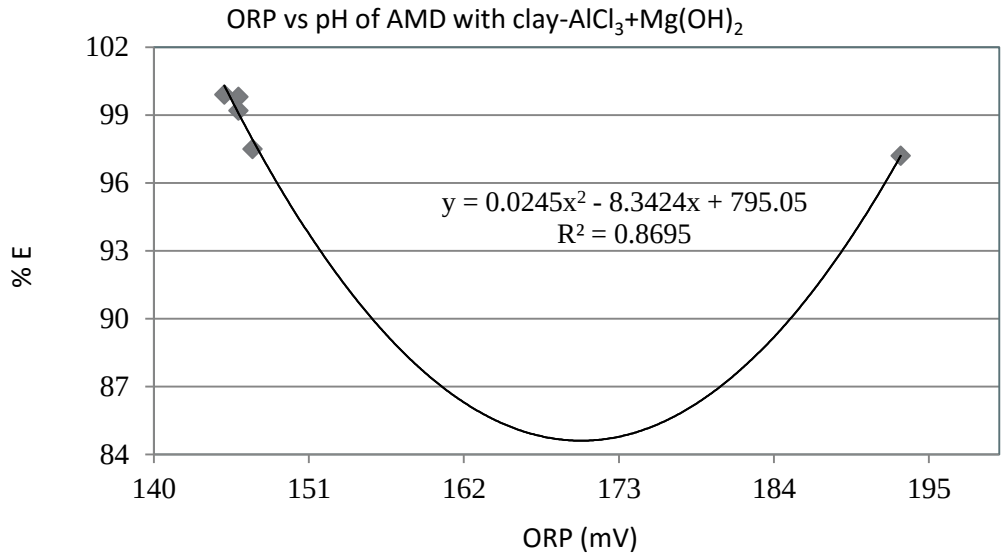
ORP vs pH of AMD with clay-AlCl3+Mg(OH)2
102
99
96
93
90
87
84
% E
y = 0.0245x² - 8.3424x + 795.05
R² = 0.8695
140
151
162
173
184
195
ORP (mV)

Fig. 9

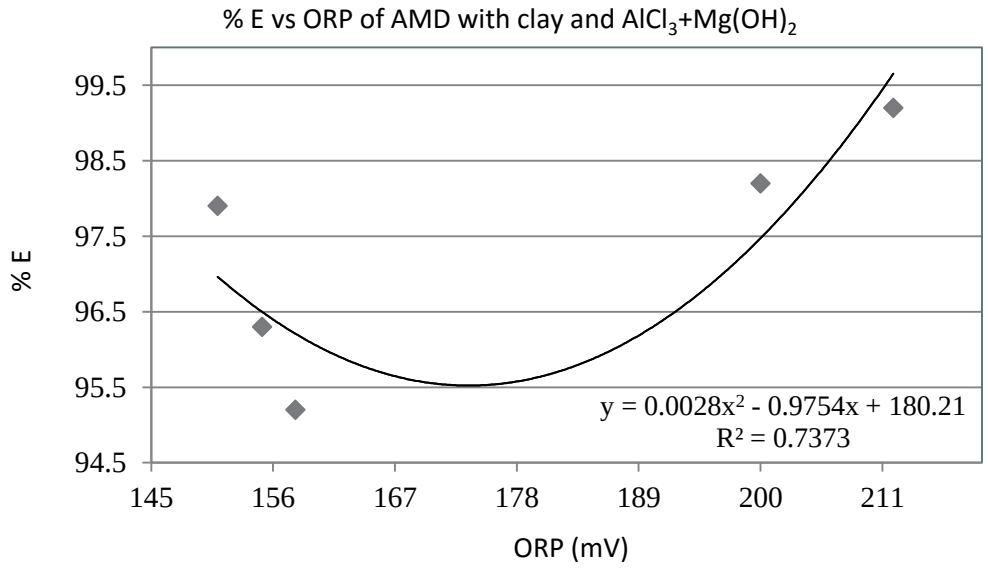
% E vs ORP of AMD with clay and AlCl3+Mg(OH)2
99.5
98.5
97.5
96.5
95.5
94.5
% E
y = 0.0028x² - 0.9754x + 180.21
R² = 0.7373
145
156
167
178
189
200
211
ORP (mV)

Fig. 10

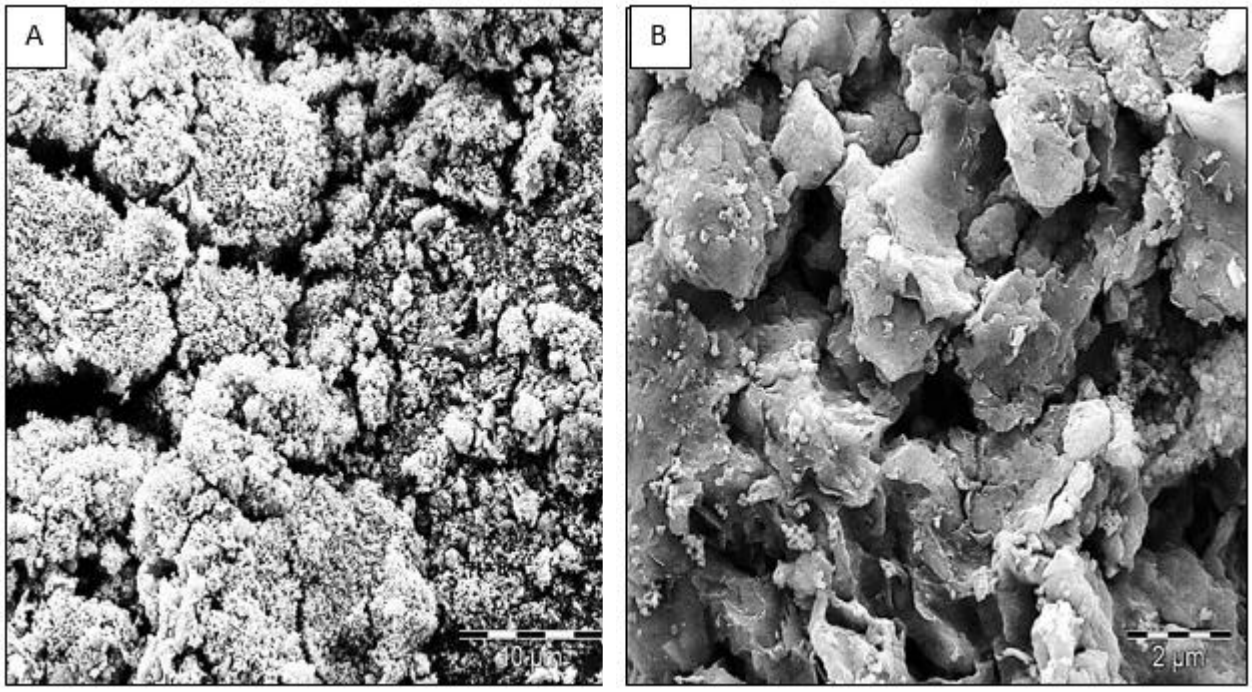

Tables

Table 1

Salt	Mass of salt (g)	Conc (mol/L)	M^{3+}conc (M)
$AlCl_3$	10.1	0.043	0.043
$Mg(OH)_2$	2.49	0.043	0.043

Table 2

Sample	pH	Conduct (mS/cm)	Turbid (NTU)	DO (mg/L)	ORP (mg/L)
Clay	2.15	2.66	13.6	5.8	230
Raw AMD	2.08	4.94	105	4.5	234